



Journal of Experimental Biology and Agricultural Sciences

<http://www.jebas.org>

ISSN No. 2320 – 8694

Antibacterial Effect of Green Synthesized Silver Nanoparticles using *Cineraria maritima*

Moorthy Duraisamy^{1*} , Santhoshkumar. S¹, Narendhirakannan R. T² ,
Ranjithkumar Rajamani³ , Ling Shing Wong⁴ , Sinouvassane Djearmane^{5*} ,
Mohamed Saleem. T.S⁶ 

¹Department of Botany, Kongunadu Arts and Science College, Coimbatore, 641 029, Tamil Nadu, India

²Department of Biochemistry, Kongunadu Arts and Science College, Coimbatore, 641 029, Tamil Nadu, India

³Viyen Biotech LLP, Coimbatore, Tamil Nadu - 641 031, India

⁴Life Science Division, Faculty of Health and Life Sciences, INTI International University, Nilai, 71800 Malaysia

⁵Department of Biomedical Science, Faculty of Science, Universiti Tunku Abdul Rahman, Kampar, 31900, Malaysia

⁶College of Pharmacy, Riyadh ELM University, Riyadh, Saudi Arabia

Received – January 26, 2022; Revision – March 16, 2022; Accepted – March 29, 2022

Available Online – October 31, 2022

DOI: [http://dx.doi.org/10.18006/2022.10\(5\).1044.1052](http://dx.doi.org/10.18006/2022.10(5).1044.1052)

KEYWORDS

Cineraria maritima

Ag NPs

SEM

FTIR

Fabric

Antibacterial

ABSTRACT

Nanoparticles display entirely novel physicochemical characteristics for specific applications because of their exceptional size and shape. Owing to the present study, we reported biosynthesis, characterization and antibacterial properties of *Cineraria maritima* (*Cm*) assisted silver nanoparticles (Ag NPs). The surface plasmon vibration, crystalline structure, surface morphology, elemental composition, and possible functional molecules vibration of prepared *Cm*-Ag NPs were characterized by different instrumentation techniques. The spectrum of UV-Vis of *Cm*-Ag NPs showed maximum plasma intensity occurred around 425nm. XRD spectrum showed the face-centred cubic (FCC) nature of *Cm*-Ag NPs. The SEM image of the *Cm*-Ag NPs demonstrated a predominantly spherical shape with cluster formation of small particles to large particles with sizes ranging from 21.57 nm to 39.16 nm. EDS spectrum indicated the existence of Ag elements in *Cm*-Ag NPs. FTIR intense peaks of *Cm*-Ag NPs showed the different functional molecules such as phenol, alkene, aldehydes, and a carbonyl group. In addition, *Cm*-Ag NPs coated textile cotton fabric sample showed substantial anti-bacterial properties against a tested bacterial pathogen.

* Corresponding author

E-mail: ycdfers@gmail.com (D. Moorthy);

sinouvassane@utar.edu.my (Sinouvassane Djearmane)

Peer review under responsibility of Journal of Experimental Biology and Agricultural Sciences.

Production and Hosting by Horizon Publisher India [HPI]
(<http://www.horizonpublisherindia.in/>).
All rights reserved.

All the articles published by [Journal of Experimental Biology and Agricultural Sciences](#) are licensed under a [Creative Commons Attribution-NonCommercial 4.0 International License](#) Based on a work at www.jebas.org.



1 Introduction

Nano-technology is one of the most actively explored areas in the biomedical sector. Generally, the properties of nanoparticles can be different due to their morphology and size (Tamulya et al. 2013; Shanmugavadivu et al. 2014). Silver (Ag) is recognized as a potential antimicrobial agent that inhibits the growth of pathogenic microbes. Many studies indicated that the Ag NPs coated with textile and medical devices to control pathogenic infection. However, for the scale-up process, commercially viable, environmentally friendly with enhanced anti-microbial properties of NPs, novel approaches in the production of silver nanoparticles must be developed (Ranjithkumar et al. 2013; Roua et al. 2021). Recent reports showed that preparation of metal and metal oxide NPs using microorganisms (extracellular and intercellular) plant extract (leaf, stem, root, fruit, seeds, peel, etc.) had proven to be eco-friendly and low-cost methods (Mittal et al. 2013; Joud et al. 2021; Das et al. 2022). In comparison with other biological routes that have been developed so far using bacteria, fungi, and algae, the plant extract-assisted Ag NPs have several advantages including scaled-up, low cost, and reaction time (Selvaraj et al. 2014; Paulkumar et al. 2021; Kavitha et al. 2021).

The mechanism of biosynthesis of NPs mostly involves bioreduction using microbial intracellular and extracellular enzymes or the plant phyto-compounds present in leaves, stems, flowers, seeds, fruits, or peels (Figure 1). So far, different medicinal plants extracts such as *Cymbopogon citrates*, *Aloe vera*, *Adiantum capillus-veneris*, *Azadirachta indica*, *Memecylon edule*,

Magnolia kobus, *Rhinacanthus nasutus*, *Morinda tinctori*, *Phyllanthus emblica*, *Malus domestica*, etc., had been used to synthesize Ag NPs and these NPs showed significant biomedical applications (Chandran et al. 2006; Elavazhagan and Arunachalam 2011; Masurkar et al. 2011; Lee et al. 2013; Lalitha et al. 2013; Pasupuleti et al. 2013; Saini et al. 2013; Santhoshkumar and Nagarajan 2014; Roy et al. 2014; Vanaja et al. 2014; Rihab et al. 2021; Netra et al. 2022). For centuries, *Cineraria maritima* has been used in the homeopathic system to treat cataracts and other severe eye-related conditions such as conjunctivitis, opacity, and corneal clouding. It is an Asteraceae family annual exotic medicinal shrub (Durgapal et al. 2021). There have been very few studies on the use of *C. maritima* whole plant extract for the biosynthesis of nanoparticles. Hence, this study was carried out to biosynthesize Ag NPs using whole plant powder extract of *C. maritima* and to evaluate the antibacterial properties of these nanoparticles.

2 Materials and Methods

2.1 Preparation of whole plant extract

Fresh plant of *C. maritima* powder was obtained from Homeopathic Research Institute at Emerald, South India. About 10 g of whole plant powder of *C. maritima* was mixed with 100 mL of deionized water and boiled for 30 minutes and the obtained crude *C. maritima* extract. After that, the crude extract of *C. maritima* was filtered using Whatman No.1 filter paper to obtain the extract of *C. maritima*.

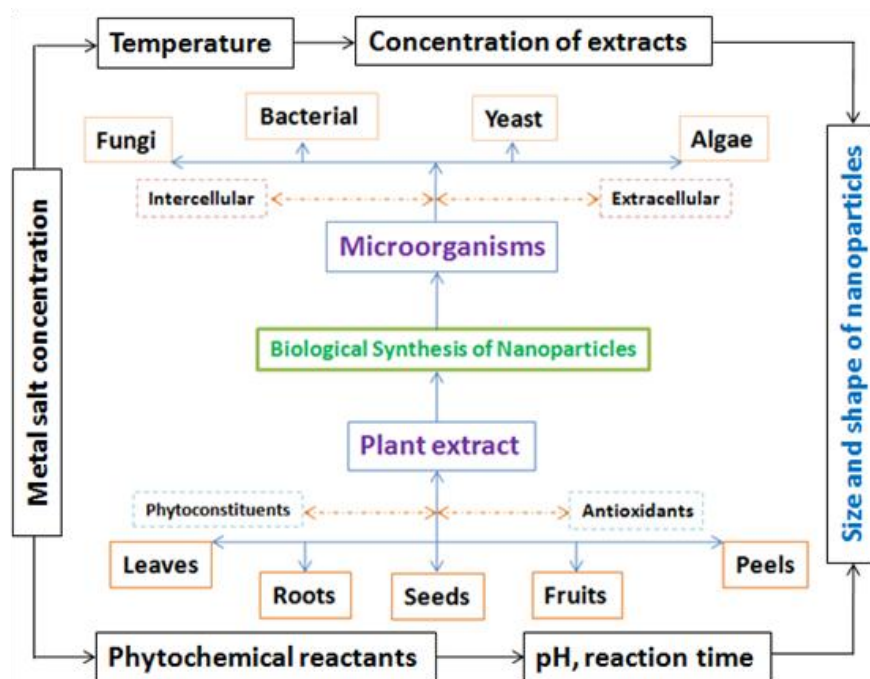


Figure 1 Source of biological substance for NPs synthesis

2.2 Biosynthesis of *Cm*-Ag NPs

About 1mM aqueous solution of 90 mL AgNO_3 was added into 10 mL of crude extract of *C. maritima* and the reaction vessel was kept in a dark condition for one day. After that, the reaction mixture was centrifugation for 30 minutes at 6000 rpm to collect *Cm*-Ag NPs. Pellets were washed with deionized water and then dried and stored for further processing.

2.3 Characterization of *Cm*-Ag NPs

The reduction of *Cm*-Ag NPs ions was observed by measuring the surface plasmon resonance (SPR) by UV-2450, Shimadzu UV-Vis analysis. The crystalline structure of the prepared *Cm*-AgNPs was examined by X-ray diffractometer (XRD) spectrum. The surface topology of biosynthesized *Cm*-Ag NPs was obtained by S-4500-SEM (Scanning electron microscopy) and the elemental composition of *Cm*-Ag NPs was performed by energy dispersive spectroscopy (EDS) attached with a scanning electron microscope (SEM). The functional groups of *Cm*-AgNPs were investigated using Fourier Transform infrared (FTIR) spectroscopy (Nicolet Avatar 660, USA).

2.4 Anti-bacterial activity of *Cm*-Ag NPs

The bacteria inoculum (*Escherichia coli*) was swabbed uniformly into culture plates prepared using MHA agar. Round cotton fabrics were cut with a diameter of 1.8 - 2.0 cm and the prepared *Cm*-Ag NPs (1mg/ mL) were treated on the fabric by standard dip dry methods. During dipping, fabrics were submerged in a solution containing *Cm*-Ag NPs (100 μL), pulled out of the bath, squeezed, and then air-dried. A fabric with *Cm*-Ag NPs was placed on top of the culture plates and incubated for 24 hours at 37°C. The zone of inhibition was recorded in millimeters (mm).

3 Results and Discussion

Crude aqueous extract *C. maritima* was used as a biological reducing agent in the production of *Cm*-Ag NPs in this investigation. The reaction mixture turned brown after 24 hours of incubation, which indicated that *Cm*-Ag NPs were being biosynthesized (Figure 2A). The biosynthesis of Ag NPs in the reaction mixture is shown by the SPR peak, which showed at 425-430 nm (Figure 2B). In general, in the surface plasma resonance phenomena, Ag NPs in an aqueous solution have a dark yellowish-

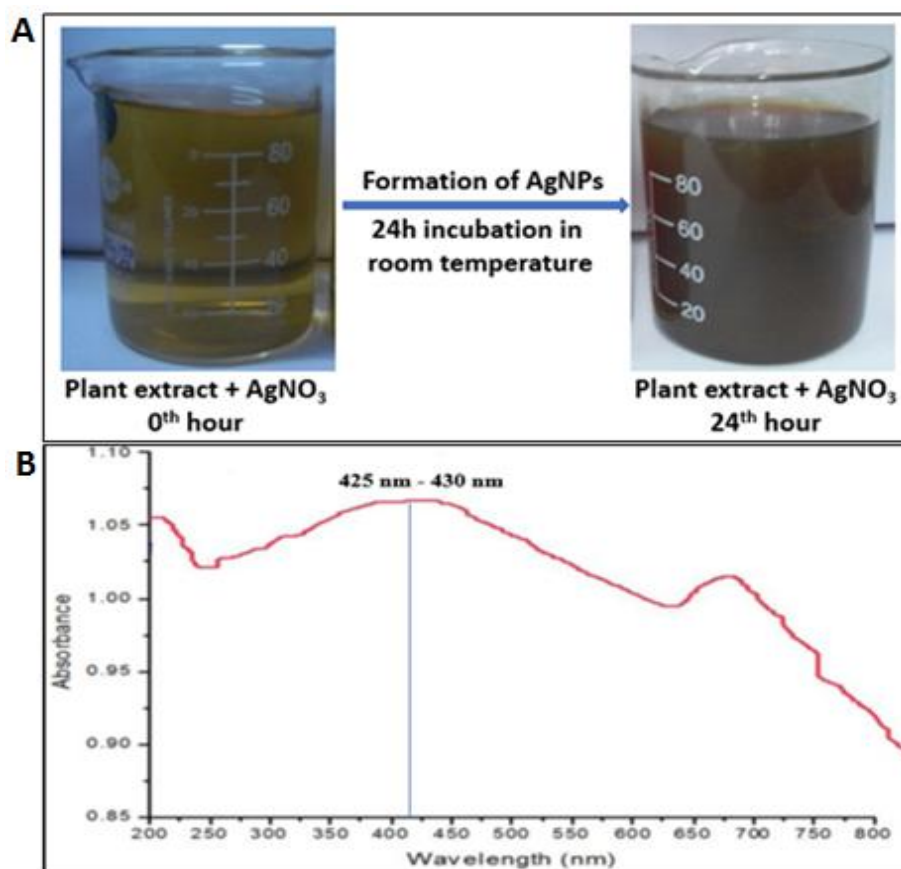


Figure 2 Biosynthesis of *Cm*-Ag NPs (A) Colour change of *Cm*-AgNPs aqueous solution, (B) Optical spectrum of colloidal solution of *Cm*-Ag NPs using UV-Vis analysis

brown color. Plant extract-assisted biogenesis Ag NPs colloidal solution was validated by UV-Vis spectrum analysis, with intensity peaks around 400 nm-450 nm (Krishnaraj et al. 2010; Chhange et al. 2011;). Similarly, in the current study the SPR peak of *Cm*-Ag NPs was around 430 nm.

The XRD spectrum of *Cm*-Ag NPs revealed prominent peaks that corresponded to the Miller indices [hkl] of silver (111), (200), (211), (220), and (311), indicating that *Cm*-Ag NPs are face-centered cubic (FCC). In addition, the XRD pattern revealed silver oxide Miller indices [hkl] of (100) and (110), orientation to JCPDS card no 04-0783, and the observed Miller indices [hkl], the observed peaks at $2\theta = 38.79^\circ, 46.48^\circ, 64.68^\circ,$ and 85.13° location suggest a synthesis of silver. In addition, regarding JCPDS file no 00-076-1393, the observed peak at $2\theta = 27.32^\circ, 32.33^\circ, 57.49^\circ,$ and 61.51° indicate the formation of silver oxide (Figure 3).

In general, the plant has a variety of phytochemicals that are responsible for NPs production through the biosynthesis method. Earlier reports suggested that the plant extract-assisted biogenesis Ag and Ag₂O exhibited X-Ray diffraction intensity at 2θ of $27^\circ, 32^\circ, 38^\circ, 44^\circ, 49^\circ, 57^\circ, 61^\circ, 64^\circ$ and 72° (Vijaya Raj et al. 2012; Awwad et al. 2013; Rufen et al. 2019). Correspondingly, the Bragg reflections pattern of XRD of the current study confirmed the presence of silver in prepared *Cm*-Ag NPs. The XRD image with additional peaks (*) may be due to the crystallization of the plant phytochemicals phase. Through the XRD pattern using the Scherrer equation (Madhan et al. 2021), the prepared *Cm*-Ag NPs revealed a particle size of around 18.36 nm to 36.15 nm.

The surface morphology of the prepared *Cm*-Ag NPs was visualized using a SEM image (Figure 4A). The topology images

of *Cm*-Ag NPs revealed that the surface morphology was not well defined; however, the prepared *Cm*-Ag NPs are predominantly spherical with cluster formation of small particles to large particles with particles size of *Cm*-Ag NPs around 21.57 nm to 39.16 nm.

The surface topology such as the size and shape of NPs showed crucial functions in the applications of NPs in different sectors (Sharmila et al. 2019; Mitchell et al. 2021). The elemental composition of *Cm*-Ag NPs was determined using their corresponding EDS spectra in this investigation, the obtained *Cm*-Ag NPs showed a peak at 3.27 keV corresponding to the binding energies of Ag ions (Figure 4B). There were also additional small peaks in the EDS spectra, indicating the presence of trace element precipitates in the *C. maritima* whole plant extract. The weight percentage of *Cm*-Ag NPs from the whole plant extract *C. maritima* was reported around 67.60 %.

FTIR analysis of *Cm*-Ag NPs shows many peaks, which indicate different functional molecules involved in the surface of the prepared sample (Figure 5). The bands observed at $3869.20\text{ cm}^{-1}, 3726.27\text{ cm}^{-1}, 3606.89\text{ cm}^{-1}, 2879.72\text{ cm}^{-1}, 1514.12\text{ cm}^{-1}, 1463.97\text{ cm}^{-1}, 999.13\text{ cm}^{-1}$ and 678.94 cm^{-1} were allotted to the vibrations of N-O, C=O, C=C, O-H, C-H, and N-H, corresponding to functional groups of carbonyl groups, cis-disubstituted alkene, phenol, carboxylic acids, aldehydes, alkene, hydroxyl, secondary amide, and alcohol. The existence of C-H, O-H, N-H, and C-C vibrations of carboxylic, hydroxyl, amine, and aromatic groups in the plant extract mediated Ag NPs was shown by FTIR intense peaks at $3422\text{ cm}^{-1}, 2921\text{ cm}^{-1}, 1743\text{ cm}^{-1}, 1631\text{ cm}^{-1}, 1240\text{ cm}^{-1}$ and 1043 cm^{-1} (Kumari et al. 2016) and these phytochemicals act as a reduction, capping and stabilization agents.

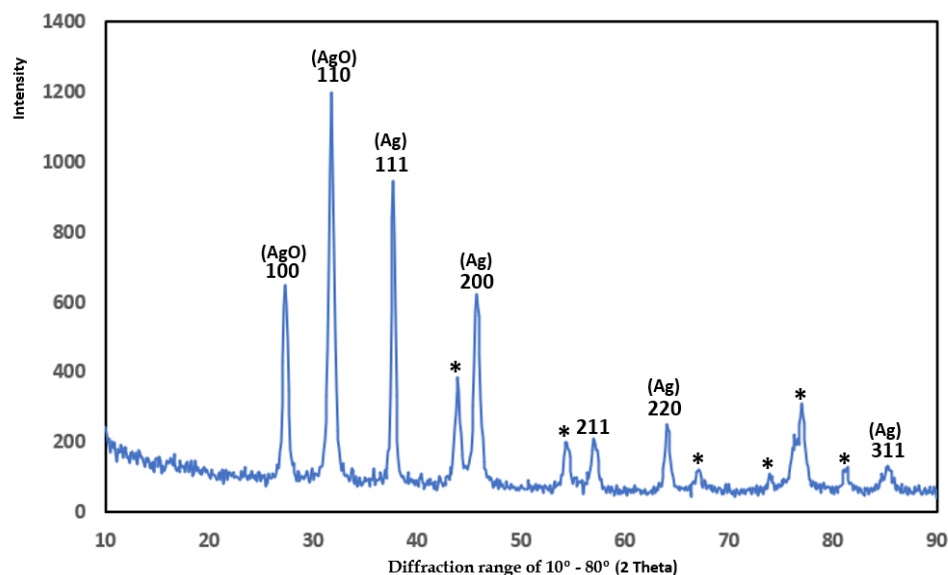
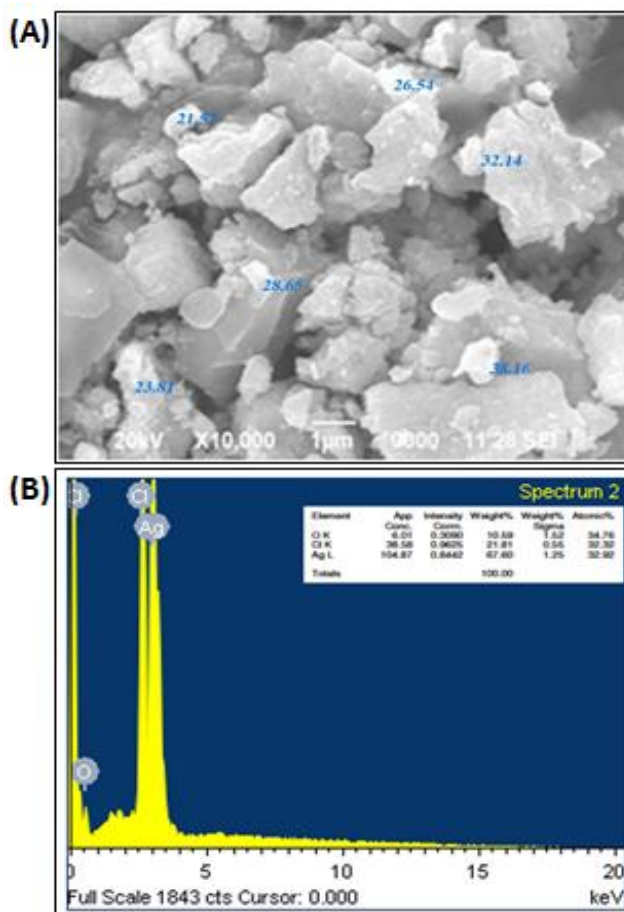
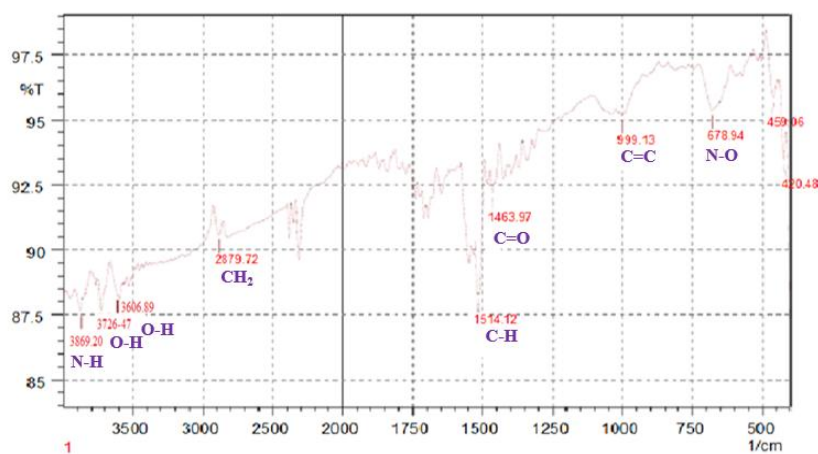


Figure 3 XRD spectrum of *Cm*-AgNPs

Figure 4 SEM-EDS analysis of *Cm*-AgNPsFigure 5 FTIR spectrum of *Cm*-Ag NPs

The FTIR spectrum revealed that the prepared *Cm*-Ag NPs contain different types of functional groups in the whole plant aqueous extract of *C. maritima* (Table 1). The phytochemicals found in the plant extract are the reason for the reduction of silver nitrate into *Cm*-Ag NPs.

Ag NPs are the most effective anti-bacterial agents when compared to another metal oxide NPs (Liao et al. 2019; Urnuksaikhon et al. 2021). The anti-bactericidal activity of *Cm*-Ag NPs fabricated fabric sample was demonstrated in this study, which showed considerable growth inhibition properties against the test pathogen

Table 1 Functional groups from FTIR spectrum of Cm-Ag NPs

| Absorption (cm^{-1}) | Molecular motion | Functional group |
|---------------------------------|-------------------------------|---|
| 3869→3606 | O-H with N-H stretching modes | Alcohol, secondary amide, hydroxyl |
| 2879 | CH_2 vibration | Alkene, aldehydes |
| 1514→1463 | C-H, C=O stretching | Carboxylic acids, phenol |
| 999→678 | C-H, C=O stretching | cis disubstituted alkene carbonyl group |

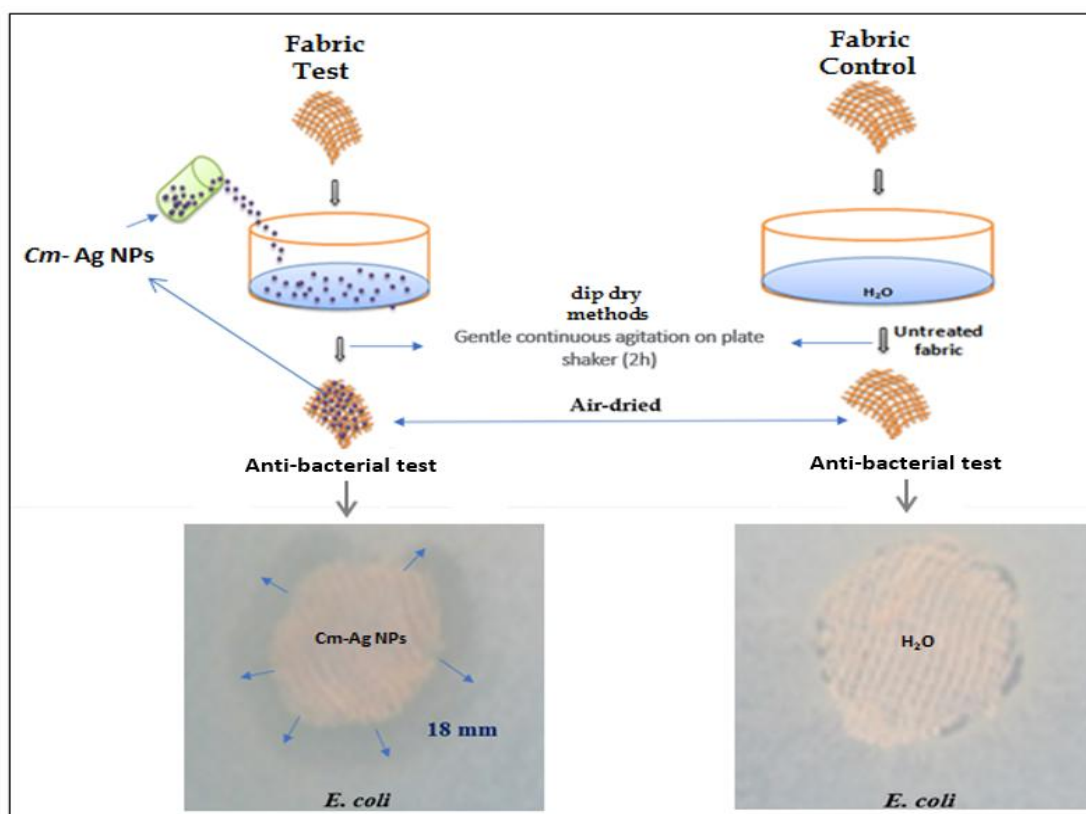


Figure 6 Antibacterial Activity of AgNPs coated fabric

of *E. coli*. Figure 6 shows the anti-bacterial activity of *Cm*-Ag NPs treated and untreated cotton fabric samples. An earlier study on the anti-bacterial properties of spherical-shaped Ag NPs produced from leaf extract of *Psidium guajavu* with particle size around 55 nm exhibited significant results against *S. aureus* and *E. coli* (Sharmila et al. 2018).

Different processes could be involved in the anti-bacterial properties of NPs such as the interaction of NPs on the surface of the bacteria cell membrane, ribosome disassembly, inactivation of essential enzymes, which are involved in the protein synthesis, NPs interact with cell signaling, etc. Nevertheless, the anti-bacterial effects of NPs are mostly determined by the size, shape, and kind of capping agent present on the NP's surface (Francis et al. 2020; Gupta et al. 2021). In the present study, the prepared *Cm*-Ag NPs coated fabric sample demonstrated a significant anti-

bacterial effect on *E. coli*, the zone of inhibition was 18 mm, whereas, the uncoated fabric sample had no inhibition zone and hence it can be used to treat and manage a wide range of microbial infections.

Conclusion

The presence of diverse active phyto-molecules in the prepared *C. Maritima* extracts resulted in the biogenesis *Cm*-Ag NPs which exhibited a brown colour in an aqueous solution and revealed an optical density peak of about 430 nm, indicating the formation of *Cm*-Ag NPs in aqueous solution. XRD spectrum indicated FCC configuration of *Cm*-Ag NPs and silver oxide NPs, and the silver oxide nanoparticles were further reduced to silver nanoparticles. The SEM image showed that the prepared *Cm*-Ag NPs have predominantly spherical surface morphology with the particle size

around 21.57 nm to 38.16 nm. EDS spectrum revealed the presence of Ag in the prepared sample. The FTIR spectrum disclosed the functional groups of alcohol, secondary amide, hydroxyl, alkene, aldehydes, carboxylic acids, phenol, cis-disubstituted alkene, and carbonyl groups. The bioreduction of Cm-Ag NPs may be due to active phytochemicals found in the aqueous extract of *C. maritima*. The findings show that the predominantly spherical shape Cm-Ag NPs had significant antibacterial efficacy against *E. coli*.

Conflicts of interest

The authors affirm that they do not have any conflict of interest.

References

- Awwad, A.M., Salem, N. M., & Abdeen, A. O. (2013). Green synthesis of silver nanoparticles using carob leaf extract and its antibacterial activity. *International Journal of Industrial Chemistry*, 4, 29. <https://doi.org/10.1186/2228-5547-4-29>
- Chandran, S. P., Chaudhary, M., Pasricha, R., Ahmad, A., & Sastry, M., (2006). Synthesis of gold nanotriangles and silver nanoparticles using *Aloe vera* plant extract. *Biotechnology Progress*, 22(2), 577-583. <https://doi.org/10.1021/bp0501423>
- Chhangte, V., Samuel, L., Ayushi, B., Manickam, S., et al. (2011). Green synthesis of silver nanoparticles using plant extracts and their antimicrobial activities: a review of recent literature. *RSC Advance*, 11, 2804-2837. <https://doi.org/10.1039/D0RA09941D>
- Das, P., Dutta, T., Manna, S., Loganathan, S., & Basak, P. (2022). Facile green synthesis of non-genotoxic, non-hemolytic organometallic silver nanoparticles using extract of crushed, wasted, and spent *Humulus lupulus* (hops): Characterization, antibacterial, and anti-cancer studies. *Environmental research*, 204(Pt A), 111962. <https://doi.org/10.1016/j.envres.2021.111962>
- Durgapal, S., Juyal, V., & Verma, A. (2021). In vitro antioxidant and ex vivo anti-cataract activity of ethanolic extract of *Cineraria maritima*: a traditional plant from Nilgiri hills. *Future Journal of Pharmaceutical Science*, 7, 105. <https://doi.org/10.1186/s43094-021-00258-8>
- Elavazhagan, T., & Arunachalam, K. D. (2011). *Memecylon edule* leaf extract mediated green synthesis of silver and gold nanoparticles. *International Journal of Nanomedicine*, 6, 1265-1278. <https://doi.org/10.2147/IJN.S18347>
- Francis, J.O., Ali, A., Idris, Y., Ayfer, A., et al. (2020). Size and shape-dependent antimicrobial activities of silver and gold nanoparticles: A model study as potential fungicides. *Molecules*, 25(11), 2682. <https://doi.org/10.3390/molecules25112682>
- Gupta, P.K., Palanisamy, S., Gopal, T., Rajamani, R., et al. (2021). Synthesis and characterization of novel Fe₃O₄/PVA/Eggshell hybrid nanocomposite for photodegradation and antibacterial activity. *Journal of Composite Science*, 5, 267. <https://doi.org/10.3390/jcs5100267>
- Joud, J., Wassim, A., Adawia, K., & Rawaa, Al. K. (2021). Green synthesis of silver nanoparticles using aqueous extract of *Acacia cyanophylla* and its antibacterial activity. *Heliyon*, 7(9), e08033. <https://doi.org/10.1016/j.heliyon.2021.e08033>
- Kavitha, A., Shanmugan, S., Awuchi, C. G., Kanagaraj, C., & Ravichandran, S. (2021). Synthesis and enhanced antibacterial using plant extracts with silver nanoparticles: Therapeutic application. *Inorganic Chemistry Communications*, 134, 109045. <https://doi.org/10.1016/j.inoche.2021.109045>
- Krishnaraj, C., Jagan, E. G., Rajasekar, S., Selvakumar, P., et al. (2010). Synthesis of silver nanoparticles using *Acalypha indica* leaf extracts and its antibacterial activity against water borne pathogens. *Colloids Surfaces B: Biointerfaces*, 76 (1), 50-56. <https://doi.org/10.1016/j.colsurfb.2009.10.008>
- Kumari, J., Mamta, B., & Ajeet, S. (2016). Characterization of silver nanoparticles synthesized using *Urtica dioica* Linn. leaves and their synergistic effects with antibiotics. *Journal of Radiation Research and Applied Sciences*, 9(3), 217-227. <https://doi.org/10.1016/j.jrras.2015.10.002>
- Lalitha, A., Subbaiya, R., & Ponnuragan, P. (2013). Green synthesis of silver nanoparticles from leaf extract *Azhadirachta indica* and to study its anti-bacterial and antioxidant property. *International Journal of Current Microbiology and Applied Sciences*, 2(6), 228-235.
- Lee, H., Song, J. Y., & Kim, B.S. (2013). Biological synthesis of copper nanoparticles using *Magnolia kobus* leaf extract and their antibacterial activity. *Journal of Chemical Technology & Biotechnology*, 88(11), 1971-1977. <https://doi.org/10.1002/jctb.4052>
- Liao, S., Zhang, Y., Pan, X., Zhu, F., et al. (2019). Antibacterial activity and mechanism of silver nanoparticles against multidrug-resistant *Pseudomonas aeruginosa*. *International Journal of Nanomedicine*, 14, 1469-1487. <https://doi.org/10.2147/IJN.S191340>
- Madhan, G., Begam, A. A., Varsha, L. V., Ranjithkumar, R., & Bharathi, D. (2021). Facile synthesis and characterization of chitosan/zinc oxide nanocomposite for enhanced antibacterial and photocatalytic activity. *International Journal of Biological Macromolecules*, 190(1), 259-269. <https://doi.org/10.1016/j.ijbiomac.2021.08.100>

- Masurkar, S. A., Chaudhari, P. R., Shidore, V. B., & Kamble, S. P. (2011). Rapid biosynthesis of silver nanoparticles using *Cymbopogon citratus* (lemongrass) and its antimicrobial activity. *Nano-Micro Letters*, 3, 189-194. <https://doi.org/10.1007/BF03353671>
- Mitchell, M. J., Billingsley, M. M., Haley, R. M., Wechsler, M. E., et al. (2021). Engineering precision nanoparticles for drug delivery. *Nature Reviews Drug Discovery*, 20, 101-124. <https://doi.org/10.1038/s41573-020-0090-8>
- Mittal, A. K., Chisti, Y., & Banerjee, U. C. (2013). Synthesis of metallic nanoparticles using plant extracts. *Biotechnology Advances*, 31(2), 346-356. <https://doi.org/10.1016/j.biotechadv.2013.01.003>
- Netra, P. N., Amit, K. K., Abhishek, K. K., Habibullah, K., et al. (2022). Anti-bacterial efficacy of bio-fabricated silver nanoparticles of aerial part of *Moringa oleifera* lam: Rapid green synthesis, In-Vitro and In-Silico screening. *Biocatalysis and Agricultural Biotechnology*, 39, 102229. <https://doi.org/10.1016/j.bcab.2021.102229>
- Pasupuleti, V. R., Prasad, T. N. V. K. V., Shiekh, R. A., Balam, S. K., et al. (2013). Biogenic silver nanoparticles using *Rhinacanthus nasutus* leaf extract: synthesis, spectral analysis, and antimicrobial studies. *International Journal of Nanomedicine*, 8, 3355-3364. <https://doi.org/10.2147/IJN.S49000>
- Paulkumar, K., Parvathiraja, C., Jesi Reeta, T., Gnanajobitha, G., et al. (2021). Green synthesis of antibacterial and cytotoxic silver nanoparticles by *Piper nigrum* seed extract and development of antibacterial silver-based chitosan nanocomposite. *International Journal of Biological Macromolecules*, 189(31), 18-33. <https://doi.org/10.1016/j.ijbiomac.2021.08.056>
- Ranjithkumar, R., Selvam, K., & Shanmugavadivu, M. (2013). Antimicrobial coated textile via biogenic synthesis silver nanoparticles. *Journal Green Science Technology*, 1(2), 111-113.
- Rihab, D., Badiia, E., Hédia, H., Ghada, B. K., et al. (2021). Biosynthesized silver nanoparticles using *Anagallis monelli*: Evaluation of antioxidant activity, antibacterial and antifungal effects. *Journal of Molecular Structure*, 1251, 132076. <https://doi.org/10.1016/j.molstruc.2021.132076>
- Roua, A., Hajera, T., Manal, A., Rabaan, A. A., et al. (2021). Green synthesis, characterization, enhanced functionality and biological evaluation of silver nanoparticles based on *Coriander sativum*. *Saudi Journal of Biological Sciences*, 28(4), 2102-2108. <https://doi.org/10.1016/j.sjbs.2020.12.055>
- Roy, K., Sarkar, C. K., & Ghosh, C. K. (2014). Green synthesis of silver nanoparticles using fruit extract of *Malus domestica* and study of its antimicrobial activity. *Digest Journal of Nanomaterials and Biostructures*, 9(3), 1137-1147
- Rufen, L., Zhenmin, C., Na, R., Yixuan, W., et al. (2019). Biosynthesis of silver oxide nanoparticles and their photocatalytic and antimicrobial activity evaluation for wound healing applications in nursing care. *Journal of Photochemistry & Photobiology B: Biology*, 199, 111593. <https://doi.org/10.1016/j.jphotobiol.2019.111593>
- Saini, J., Kashyap, D., Batra, B., Sumit, K., et al. (2013). Microbial biotechnology green synthesis of silver nanoparticles by using neem (*Azadirachta indica*) and amla (*Phyllanthus emblica*) leaf extract. *Indian Journal of Applied Research*, 3(5), 209-210.
- Santhoshkumar, S., & Nagarajan, N. (2014). Biological synthesis of silver nanoparticles of *Adiantum capillus-veneris* L. and their evaluation of antibacterial activity against human pathogenic bacteria. *International Journal of Pharmaceutical Sciences and Research*, 5(12), 5511-5518. [http://dx.doi.org/10.13040/IJPSR.0975-8232.5\(12\).5511-18](http://dx.doi.org/10.13040/IJPSR.0975-8232.5(12).5511-18)
- Selvaraj, K., Ranjana, C., & Chiranjib, C. (2014). A green chemistry approach for the synthesis and characterization of bioactive gold nanoparticles using *Azolla microphylla* methanol extract. *Frontiers of Materials Science*, 8(2), 123-135. <https://doi.org/10.1007/s11706-014-0246-8>
- Shanmugavadivu, M., Selvam, K., & Ranjithkumar, R. (2014). Green synthesis of silver nanoparticles from pomegranate peel extract and its antimicrobial activity. *American Journal of Advance Drug Deliver*, 2(2), 174-182.
- Sharmila, C., Prabhavathi, V., Dinesh, B., Ranjithkumar, R., & Chandarshekar, B. (2019). Shape controlled synthesis of dextran sulfate stabilized silver nanoparticles: Biocompatibility and anticancer activity. *Material Research Express*, 6(4), 1-7. <https://doi.org/10.1088/2053-1591/aafefc>
- Sharmila, C., Ranjithkumar, R., & Chandarshekar, B. (2018). *Psidium guajava*: a novel plant in the synthesis of silver nanoparticles for biomedical applications. *Asian Journal of Pharmaceutical and Clinical Research*, 11(1), 341-345. <https://doi.org/10.22159/ajpcr.2018.v11i1.21999>
- Tamulya, C., Hazarika, M., Borah, S. C., Das, M. R., & Boruah, M. P. (2013). In situ biosynthesis of Ag, Au and bimetallic nanoparticles using *Piper pedicellatum* C.DC: green chemistry approach. *Colloids and Surfaces B Biointerfaces*, 102, 627-634. <https://doi.org/10.1016/j.colsurfb.2012.09.007>

- Urnukhsaikhan, E., Bold, B. E., Gunbileg, A., Sukhbaatar, N., & Mishig-Ochir, T. (2021). Antibacterial activity and characteristics of silver nanoparticles biosynthesized from *Carduus crispus*. *Scientific reports*, *11*(1), 21047. <https://doi.org/10.1038/s41598-021-00520-2>
- Vanaja, M., Paulkumar, K., Baburaja, M., Rajeshkumar, S., et al. (2014). Degradation of methylene blue using biologically synthesized silver nanoparticles. *Bioinorganic Chemistry and Application*, *2014*, 742346. <https://doi.org/10.1155/2014/742346>
- Vijaya Raj, D., Anarkali, J., Rajathi, K., & Sridhar, S. (2012). Green synthesis and characterization of silver nanoparticles from the leaf extract of *Aristolochia bracteata* and its antimicrobial activity. *International Journal of Nanomaterials and Biostructures*, *2*(2), 11-15. <https://doi.org/10.1002/bab.2235>